

Assessing the RF Performance of Medical Implant Antennas

Yomna El-Saboni, Matthew K. Magill, Gareth A. Conway, William G. Scanlon

Centre for Wireless Innovation, Queen's University of Belfast, UK

(contact: w.scanlon@qub.ac.uk)

Abstract

Active implantable medical devices are becoming increasingly more popular as new applications are developed to improve patient treatment and care. Many implant applications are utilising RF techniques to provide communication and control for electronic devices within the human body, especially at frequencies between 400 MHz and 2.45 GHz. Physical size is an obvious and important concern in the design of implant devices and this means that there is a need for innovation in the design of miniaturised antenna solutions that have adequate performance in the challenging human body environment. While there is a role for simulation and modelling, the test and characterisation of these innovative implant antennas is another crucial factor in the development of these medical systems. There are many issues to take into consideration that can affect the results obtained when testing miniaturized implant antennas. For example, the local environment surrounding the antenna affects both impedance matching and radiation performance and so the test environment, typically a tissue equivalent phantom, is extremely important. Additionally, in practice the close proximity of the body tissues affects the antenna's radiation performance and introduces significant losses into the reactive near fields that are associated with resonant antennas. This highlights not only the importance of accurate phantom modelling and the effect of antenna coating material, but also the source feeding techniques and characterizing its sensitivity inside the phantom.

This paper will specifically illustrate the challenges faced when conducting radiation efficiency measurements for implantable antennas when they are inserted inside a tissue representative human body phantom. Our objective is to highlight the disturbance caused by the necessary feed cable and demonstrate techniques to minimize it. Only standardized antennas were used and the measurements were conducted using a novel reverberation chamber approach to obtain highly accurate results at extremely low radiation efficiencies associated with these applications. In order to gain a better understanding, the experiment was repeated with different antennas and phantom set ups and the results clearly illustrate the factors that need to be considered when assessing the RF performance of medical implant antennas.

1. Radiation Efficiency Measurements

A standardized element in the testing of implantable antennas and their performance which often does not receive the attention that it deserves is radiation efficiency. Most emphasis in performance characterization of implanted antennas illustrated in the literature has been on the reflection coefficient, bandwidth, and far-field radiation pattern [1]. Nonetheless, the topic has received some attention including [2] where the authors conducted simulations to estimate implanted antenna radiation efficiency in different antennas. However, it remains extremely difficult to empirically evaluate implant antenna efficiency, primarily because of the extremely low efficiency values

involved, often around 1% or less (depending on the implantation 'depth' within a lossy tissue equivalent phantom). This is the motivation for the current work where consider if a reverberation chamber based approach can be used for the measurement of implant antenna radiation efficiency.

Any antenna radiation efficiency measurement is subject to a range of errors that can reduce accuracy and repeatability and this also applies to the reverberation chamber technique which is based on a statistical characterisation of the radiation from the antenna under test (AUT) having being placed within a tissue equivalent phantom (to represent the human body lossy tissue environment) with the chamber losses being calibrated out using a reference load.

Nonetheless, with the reverberation chamber approach the use of a Vector Network Analyzer (VNA) already ensures a high standard of performance with the usual experimental techniques to help improve measurement accuracy and reduce systematic measurement errors [3]. Yet, there are many other factors that can disturb the results obtained from implant/phantom testing, one of which is the experimental setup as it involves the use of a coaxial cable to feed the implantable antenna inside the phantom. Feeding an implantable antenna in an efficient manner can be very challenging, mainly because impedance measurements are affected [4]. A perfectly balanced structure cannot be established with a miniaturized antenna as anything mounted on a small antenna will contribute to the overall radiation and the currents will radiate outside the coaxial cable [5]. This is a major concern for implanted antenna efficiency measurements since the typically low efficiency of the antenna means that any spurious radiation from the feed cable may be more significant.

Moreover, the reflection coefficients measured using the VNA are highly dependent on the length of the coaxial cable used to feed the antenna inside the phantom [3]. Because the experimental setup used to study the propagation or the behaviour of an implantable antenna requires the use of long flexible cables that can go down the phantom container, the losses are potentially higher. Usually, the effect of the cable can be negligible, but due to the physically small size and the extreme sensitivity of the results, this effect should be analysed in order to minimize or eliminate it. Although this may not affect a functioning implant inside a human body (which does not require a feed cable) it does affect the measurements obtained from prototype testing and so must be carefully considered.

To address this issue, one study looked briefly at the cable effects by testing two scenarios where the antenna is placed in an empty phantom and when it is placed in a filled liquid phantom where the cable is in direct contact with the liquid [6]. They conducted their analysis in the 403 MHz band and verified the results through simulations. They studied the reflection coefficient (S_{11}) of the antenna and noted how the cable can have a considerable impact on the empirical results. However, their study did not consider the impact of the feeding cable on the radiation efficiency measurements. Others suggested using alternatives to a coaxial cable such as an optical fibre. In one study, optical fibres have been utilized to estimate the characteristics of a monopole antenna where they connected the fibre optic to RF transducer and powered by DC voltage [5]. They measured the noise level, dynamic range and the frequency response and compared it the results obtained using a coaxial cable. Their results clearly show a difference between both techniques and it seems that the fibre optics are more efficient. However, the study does not show details of the experimental setup implemented with a coaxial cable.

2. Frequency of operation

Choosing a suitable operating frequency is very important when it comes Implantable medical devices. Currently, the IEEE Std 802.12.6 2012 standardized the communication channels and the wireless interconnection between all the biomedical nodes forming any body area network (BAN). This is an international standard that implements industrial scientific medical (ISM) frequency bands and other approved band by national medical and/or regulatory authorities [7]. This standard clearly establishes the physical layer for the short range wireless communication between wearable, implantable or close to body devices. There are several frequency bands utilized in BANs however, the most used so far is

the medical implant communication services (MICS) band i.e., 402-405MHz [8]. Because this band lies in the lower frequency ranges, when compared with ISM bands, MICS has less signal attenuation and wave propagation losses as the path goes through the different body tissues that exhibits different dielectric properties and have varying water contents which is a great advantage when used in implant applications [9]. However, the MICS allocation has a very narrow bandwidth and has effective isotropic radiated power (EIRP) restrictions which reduce the achievable bit rates in practical applications. To accommodate for future applications with highly intelligent and sensitive sensors and real time responsive medial systems that may require pattern recognition techniques, wider channel bandwidth must be achieved. Consequently, there has been increased interest in higher frequencies for implant applications. While body tissue losses are greater, the use of higher frequency bands enables a reduction in the physical size of the antenna and allows further miniaturization which is highly beneficial for implantable devices and enables a wider range of potential applications.

3. Phantoms

When evaluating an implant antenna or analysing its wave propagation, a human body model is required to visualize the interactions between the device and the body tissues and how they affect each other. For such investigations, human equivalent phantoms are designed with permittivity and conductivity characteristics that mimic the human tissues as much as possible. Not only phantoms rule out ethical issues associated with testing human tissue, but they also provide reproducibility of the results obtained. Human body phantoms fall under two main categories: numerical and tissue equivalent experimental phantoms [10]. Both phantoms can be developed in a single homogenous or a multi-layer fashion depending on the application and the accuracy needed. Once standardized, a numerical phantom can be easier to share, more reproducible and provides accurate properties of human tissues and a clear insight about the expected behaviour.

For implant applications, liquid based tissue equivalent phantoms are the most convenient and provide good reproducibility of results [11], [12]. The phantom specifications are highly critical, most importantly because it is modelling the human body which is considered a highly dispersive medium with different tissue shapes and frequency dependent properties [6]. There are many issues in the type of phantom that should be addressed which can directly affect the results obtained when testing a miniaturized implantable antenna. One factor widely discussed in literature and emphasized is the phantom material and how it affects the signal strength and its attenuation. In one study [13] simulations were conducted to compare the results obtained from a single layered phantom with a multi-layered phantom, taking into account the different tissue types and studying the effect of specifically the muscle, fat and skin tissue. These 3 tissues have been modelled as different layers with their corresponding permittivity and conductivity. This study shows how the gain is disturbed by changing the depth at which the antenna is placed especially when the signal has to pass through different boundaries. Due to their higher permittivity, the muscle and skin equivalent layers are more lossy and as the boundary between the two antennas increases along these layers, the gain is significantly reduced. The high permittivity and conductivity properties of the body tissues cause high propagation losses.

4. Implant Testing Methodology

In this work, only canonical antennas (a monopole and a sleeve dipole) were considered because the objective of this specific study is not to evaluate the design of the antenna, but rather to evaluate the experimental design. The antennas were uninsulated to ensure that they were highly coupled to the lossy dielectric environment in the phantom and while their radiation characteristics are well understood, due to near field material losses they are quite inefficient. Therefore, any significant change in the measured radiation efficiency highlights experimental considerations such as radiation from the AUT feed cable.

A set of 12 experiments were conducted inside the reverberation chamber and radiation efficiency measurements were captured. In all of them, the antenna was held by a rigid coaxial cable and inserted in a cylindrical liquid phantom as shown in Figure 1. Both antennas (Figure 2) were tested in muscle equivalent liquid and for each 3 different scenarios were carried out.

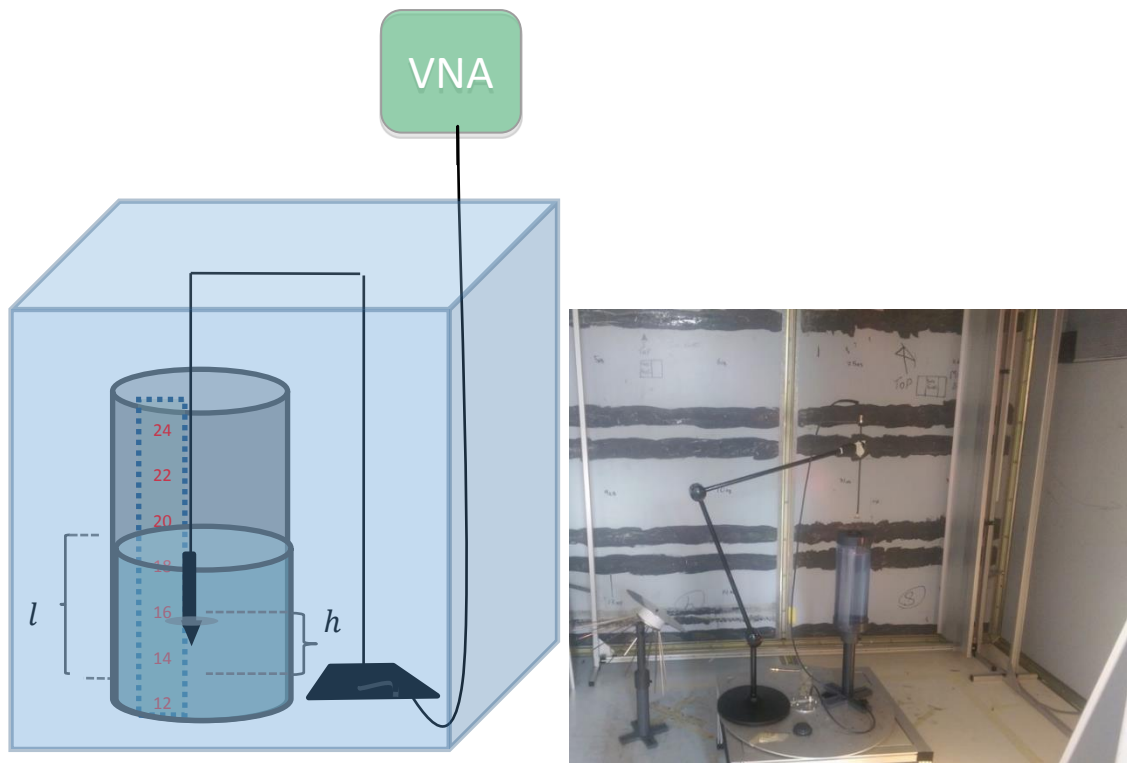


Figure 3 (left) schematic of the phantom arrangement inside the reverberation chamber, (right) an image of the experimental setup



Figure 4 Antennas used in the study (Left) monopole, (right) sleeve dipole

The efficiency results were obtained for the 2200–2300 MHz frequency range as this was optimal for both of the antenna types under investigation and it is also adjacent to the MedRadio allocation. However, the experimental technique can be applied to MICS or any other relevant frequency band depending on the specification of the reverberation chamber used. Furthermore, higher frequencies are becoming more common for medical implants as they feature increased communication bandwidth in comparison with the MICS band [14].

4.1 Reverberation Chamber

The reverberation chamber used in this study has been previously introduced in [15] and is based on a 2.4 x 2.4 x 2.4 m shielded room with fixed metallic baffles. It is equipped with a rotational table,

three antennas, two mechanical plate stirrers, polarization stirring, where the stirrers and control and data acquisition software were provided by Bluetest AB. The software settings are shown in Figure 5. For polarization stirring the chamber features wideband monopole test antennas (400 – 3000 MHz) on the roof of the chamber and two walls and the VNA used was a Rohde and Schwarz ZVB-8. The measurements were taken over a 400 MHz range from 2200–2600 MHz as shown in Figure 6. However, the radiation efficiency results presented in this paper are over a 100 MHz bandwidth from 2200 MHz as both antennas are best matched in this band.

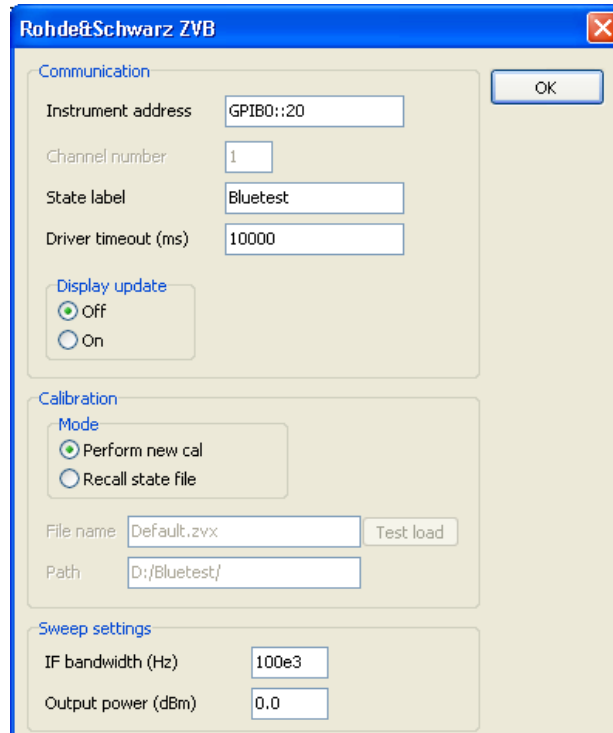


Figure 7 Bluetest file settings settings

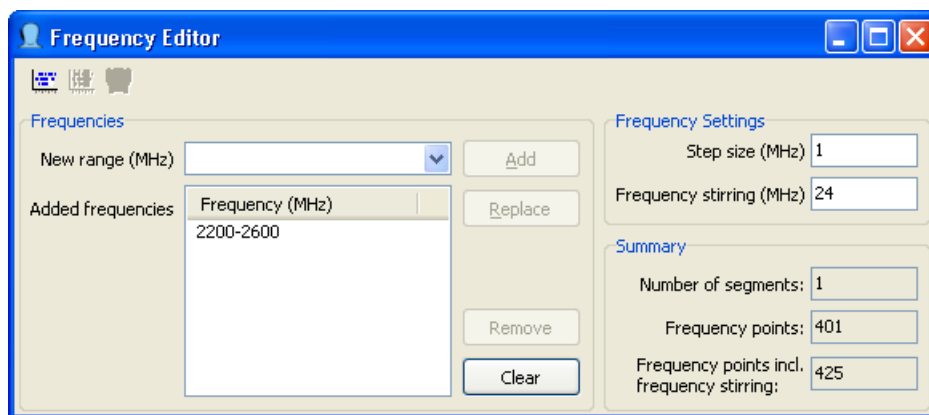


Figure 8 Frequency settings

Prior to capturing any measurements, a reference file created by connected the VNA to the discone reference antenna shown in the image in Figure 9 on the left with the settings illustrated in Figure 5. The reference measurement was taken while placing both antennas (each loaded with 50 Ω) and the full phantom inside the reverberation chamber and the file was used as a reference for all efficiency measurements conducted in this study.

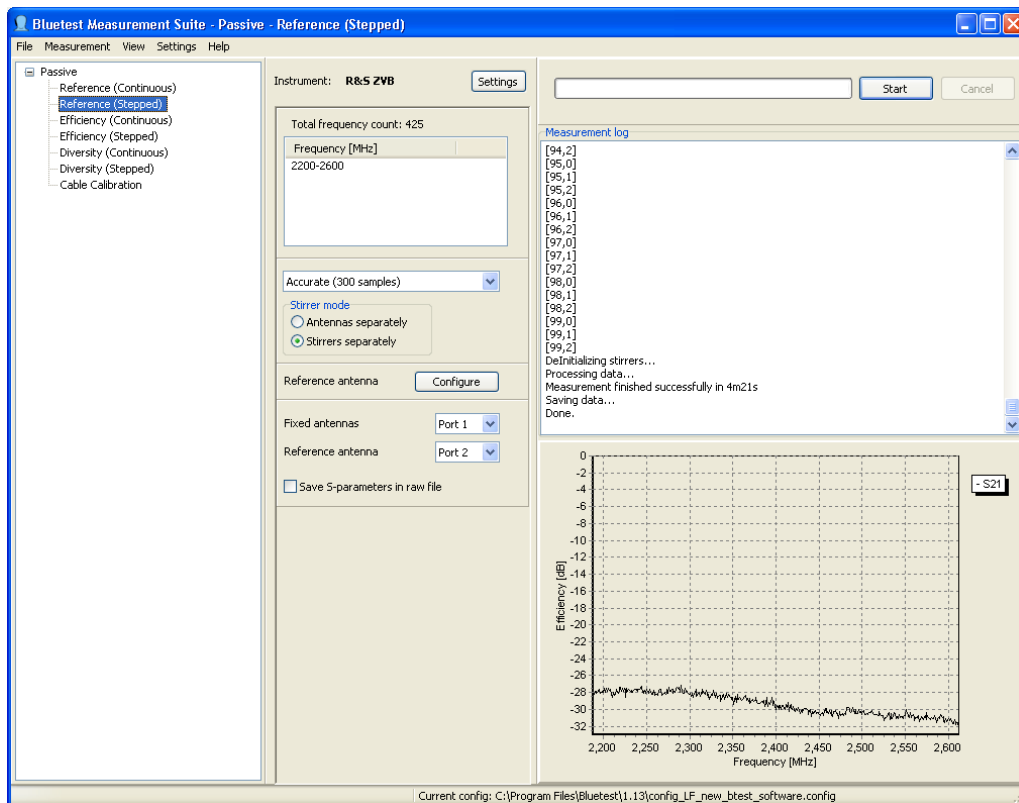


Figure 10 Bluetest reference file

4.2 Phantom characteristics

The implant antennas were tested in a rotationally symmetrical cylindrical phantom with 12 cm diameter, 28 cm length and 0.2 cm PVC wall thickness as discussed in [16] and shown in the image in Figure 1. The cylindrical phantom was filled with a lossy dielectric solution that mimics the characteristics of human muscle tissue at the mid band frequency of 2250 MHz. The muscle equivalent liquid was as used in [17] by modifying a glycol solution to exhibit a relative permittivity of 58.3 and conductivity of $1.81 \text{ S} \cdot \text{m}^{-1}$. Muscle equivalent liquid was chosen because it is one of the major tissue types in the human body and its high signal attenuation helps demonstrate the sensitivity of the reverberation chamber method.

4.3 Setup Arrangement

In all cases the AUT was connected to a 30 cm insulated rigid coaxial cable (RG405) before connection via another 1 m coaxial cable to the chamber turn table port (VNA). The coaxial cable is then immersed inside the liquid phantom as shown in Figure 11, where the antenna is held at the bottom of the cable and moves deeper inside the cylindrical phantom.

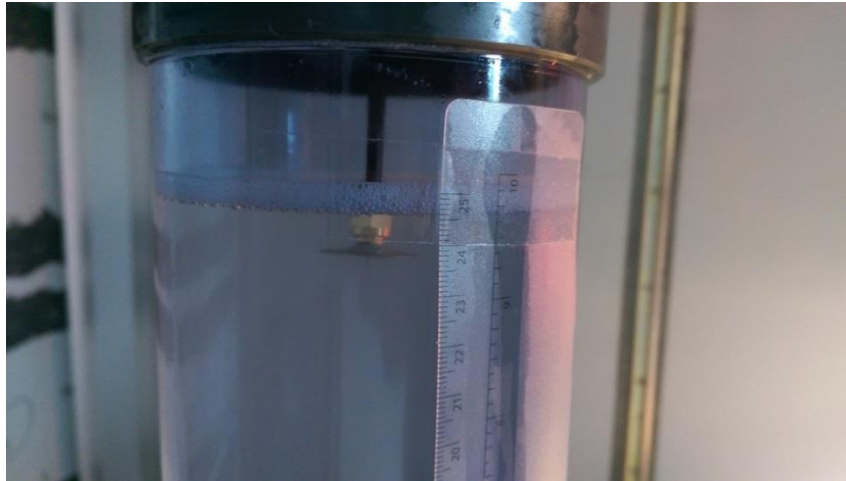


Figure 12 Positioning the antenna inside the phantom

Scenario 1 – Antenna position fixed – variable phantom height

Initially the antenna was held by a coaxial cable that is attached to an adjustable stand in a similar fashion to Figure 13. The antenna's position was fixed at the bottom of the empty phantom case with the antenna feed point 6 cm from the base of the phantom and central to the axis of the cylinder. The tissue equivalent liquid was poured gradually with 120 ml (2 cm) intervals. The efficiency was then measured using the reverberation chamber at each interval without changing the position of the antenna. Since the shortest path from the antenna to the outside of the phantom is radial and this distance does not change, any changes in measured implant antenna efficiency are related to cable effects.

Scenario 2 – Antenna positioned always in centre of the phantom but variable phantom height

The same experimental setup shown in Figure 1 was used but this time the antenna's vertical position was adjusted to stay at a mid-point to the height of the liquid in the cylinder as the volume of the liquid was gradually changing. The radiation efficiency was also measured at each interval. Compared to Scenario 1, this case helps identify the bulk absorption effect of the larger phantom, although it is also potentially subject to cable effects as well. Note that the shortest path from the antenna to the outside of the phantom is the same as Scenario 1 and this should be the dominant factor.

Scenario 3 – Full phantom – variable antenna position

The same experimental setup was used, however this time the phantom case was fully filled with the tissue equivalent liquid and remained constant throughout the experiment. The antenna's vertical position was adjusted at intervals of 2 cm each and the radiation efficiency was measured at every new position.

This experiments were conducted to illustrate the consequences of any radiation from the measurement cable inside the phantom. Additionally, these efficiency measurements demonstrate

the propagation of a single antenna placed inside a phantom and provide more insight about the path loss and signal attenuation.

5. Results and Discussion

The procedure was repeated twice and the average of both results was plotted. In the first case (Scenario 1) the measurements clearly show how the increase in liquid phantom volume reduces the total radiation efficiency with both antennas as can be shown in Figure 14. The reduction in radiation efficiency must be due to either dampening of RF currents flowing on the outside of the feed cable as the cable passes through the lossy muscle equivalent material or due to the bulk absorption associated with a greater volume of phantom material.

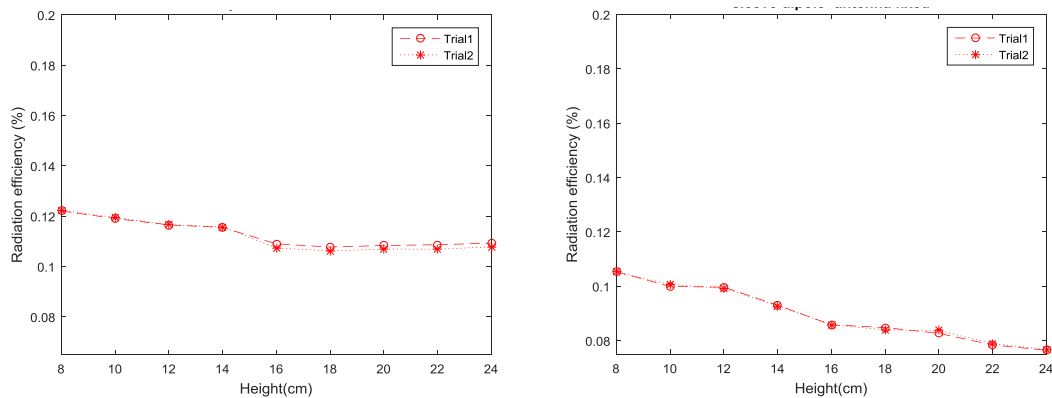


Figure 15 Total Radiation efficiency measurements of a (a) monopole, (b) sleeve dipole for Scenario 1 where the antenna is held fixed at 6 cm and the liquid level increases from 8 cm to 24 cm with 2 cm intervals.

In the second case (Scenario 2), although it is less visible, the measurements still demonstrate how the antenna has a higher radiation efficiency when the level of the liquid phantom decreases as shown in Figure 16. Again the reduction in radiation efficiency can only be due to either of the two factors mentioned above.

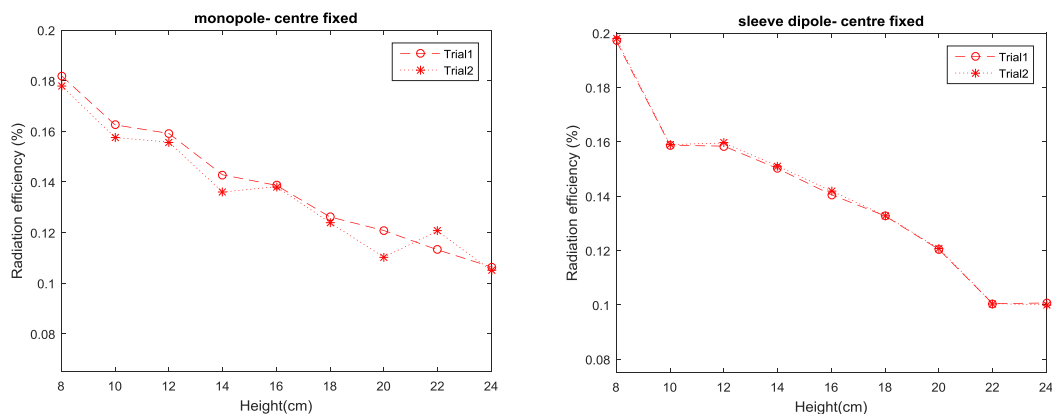


Figure 17 Total Radiation efficiency measurements of a (a) monopole, (b) sleeve dipole for Scenario 2 where the antenna is always placed at the mid point of the liquid level as it increases from 8 cm to 24 cm with 2 cm intervals and the antenna moves from 4 cm to 12 cm with 1 cm intervals.

In the third case (Scenario 3), the measurements illustrate how the antenna has a higher radiation efficiency when it the antenna is at the top than when it moves downwards as shown in Figure 18. This proves that the cable is radiating and affecting the total radiation efficiency measurement.

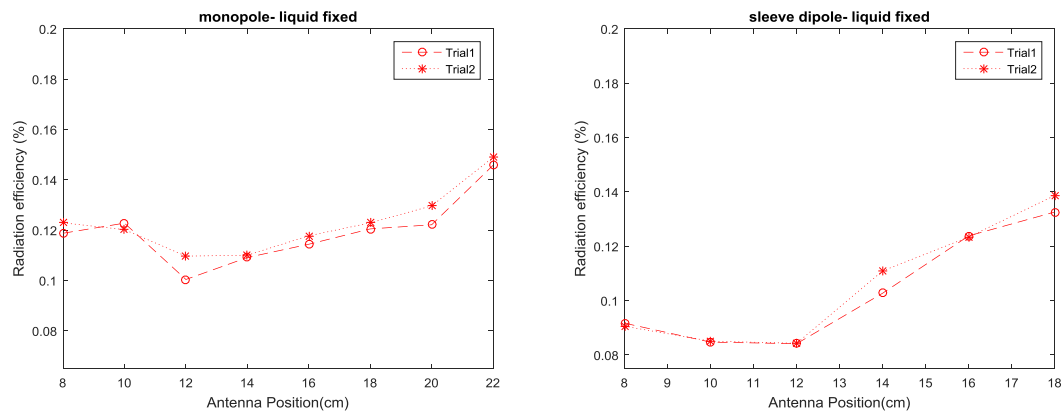


Figure 19 Total Radiation efficiency measurements of a (a) monopole, (b) sleeve dipole for Scenario 3 where the liquid level remains constant at 24 cm and the position of the antenna changes from 8 cm to 22 cm with 2 cm intervals.

6. Conclusion

This study presents a measurement technique used to estimate the radiation efficiency of deep implant antennas inside a liquid phantom. Based on the preliminary results presented, the use of the reverberation chamber illustrates a high accurate method for efficiency measurements as the results are reproducible with minimal variation ($< 0.05\%$). This study also shows that the cable radiates inside the liquid and its effect can vary depending on the antenna type. For future work, it is intended to test other antenna types with different radiation patterns to analyse ways of minimizing cable effects on the efficiency measurements.

References

- [1] A. Kiourti and K. S. Nikita, "A Review of Implantable Patch Antennas for Biomedical Telemetry: Challenges and Solutions [Wireless Corner]," *IEEE Antennas Propag. Mag.*, vol. 54, no. 3, pp. 210–228, Jun. 2012.
- [2] X. Meng, K. D. Browne, S.-M. Huang, C. Mietus, D. K. Cullen, M.-R. Tofighi, and A. Rosen, "Dynamic Evaluation of a Digital Wireless Intracranial Pressure Sensor for the Assessment of Traumatic Brain Injury in a Swine Model," *IEEE Trans. Microw. Theory Tech.*, vol. 61, no. 1, pp. 316–325, Jan. 2013.
- [3] M. Hiebel, *Fundamentals of Vector Network Analysis*. Rhode & Schwarz, 2007.
- [4] A. K. Skrivervik, J.-F. Zurcher, O. Staub, and J. R. Mosig, "PCS antenna design: the challenge of miniaturization," *IEEE Antennas Propag. Mag.*, vol. 43, no. 4, pp. 12–27, 2001.
- [5] A. Scannavini, L. J. Foged, and L. Scialacqua, "Testing electrically small antennas with using a fiber optic to RF transducer," in *2014 IEEE Antennas and Propagation Society International Symposium (APSURSI)*, 2014, pp. 271–272.
- [6] F. Merli and A. K. Skrivervik, "Design and measurement considerations for implantable antennas for telemetry applications," in *Proceedings of the Fourth European Conference on Antennas and Propagation*, 2010, pp. 1–5.
- [7] "IEEE Standard for Local and metropolitan area networks - Part 15.6: Wireless Body Area Networks," pp. 1–271, 2012.
- [8] L. Schmitt, J. Espina, T. Falck, and D. Wang, "Biosensor Communication Technology and

- Standards," in *Handbook of Biomedical Telemetry*, Hoboken, NJ, USA: John Wiley & Sons, Inc., 2014, pp. 330–367.
- [9] R. Chavez-Santiago, C. Garcia-Pardo, A. Fornes-Leal, A. Valles-Lluch, G. Vermeeren, W. Joseph, I. Balasingham, and N. Cardona, "Experimental Path Loss Models for In-Body Communications within 2.36-2.5 GHz," *IEEE J. Biomed. Heal. Informatics*, vol. 19, no. 3, pp. 1–1, 2015.
- [10] K. Ito, "Human body phantoms for evaluation of wearable and implantable antennas," in *IET Seminar Digests*, 2007, pp. 590–590.
- [11] W. Xia, K. Saito, M. Takahashi, and K. Ito, "Performances of an Implanted Cavity Slot Antenna Embedded in the Human Arm," *IEEE Trans. Antennas Propag.*, vol. 57, no. 4, pp. 894–899, Apr. 2009.
- [12] H.-Y. Lin, M. Takahashi, K. Saito, and K. Ito, "Characteristics of Electric Field and Radiation Pattern on Different Locations of the Human Body for In-Body Wireless Communication," *IEEE Trans. Antennas Propag.*, vol. 61, no. 10, pp. 5350–5354, Oct. 2013.
- [13] J. Gemio, J. Parron, and J. Soler, "Human Body effects on Implantable Antennas for ISM Bands Applications: Models Comparison and Propagation Losses Study," *Prog. Electromagn. Res.*, vol. 110, pp. 437–452, 2010.
- [14] F. Merli, L. Bolomey, J. Zürcher, E. Menville, and A. K. Skrivervik, "Versatility and tunability of an implantable antenna for telemedicine," in *Proceedings of the 5th European Conference on Antennas and Propagation (EUCAP)*, 2011, pp. 2487–2491.
- [15] G. A. Conway, W. G. Scanlon, C. Orlenius, and C. Walker, "In Situ Measurement of UHF Wearable Antenna Radiation Efficiency Using a Reverberation Chamber," *IEEE Antennas Wirel. Propag. Lett.*, vol. 7, pp. 271–274, 2008.
- [16] "Chamber Load | BLUETEST.se." [Online]. Available: <https://bluetest.se/products/accessories/chamber-load>.
- [17] G. A. Conway and W. G. Scanlon, "Antennas for Over-Body-Surface Communication at 2.45 GHz," *IEEE Trans. Antennas Propag.*, vol. 57, no. 4, pp. 844–855, Apr. 2009.